# A primary thymic adenocarcinoma with two components that traced distinct evolutionary trajectories

AUTHOR(S):

Ishida, Ayami; Yamada, Yosuke; Ishida, Yoshihiro; Yoshizawa, Akihiko; Nakajima, Daisuke; Date, Hiroshi; Marx, Alexander; Haga, Hironori

CITATION:

Ishida, Ayami ...[et al]. A primary thymic adenocarcinoma with two components that traced distinct evolutionary trajectories. Pathology International 2021, 71(12): 849-855

ISSUE DATE:

2021-12

URL:

http://hdl.handle.net/2433/276516

# A primary thymic adenocarcinoma with two components that traced distinct evolutionary trajectories

Ayami Ishida[1], Yosuke Yamada[1,*], Yoshihiro Ishida[2], Akihiko Yoshizawa[1], Daisuke Nakajima[3], Hiroshi Date[3], Alexander Marx[4], Hironori Haga[1]

[1]Department of Diagnostic Pathology, Kyoto University Hospital, Kyoto, Japan

[2]Department of Dermatology, Kyoto University Hospital, Kyoto, Japan

[3]Department of Thoracic Surgery, Kyoto University Hospital, Kyoto, Japan

[4]Institute of Pathology, University Medical Centre Mannheim and Medical Faculty Mannheim, Heidelberg University, Mannheim, Germany

***Corresponding Author**
Yosuke Yamada
Department of Diagnostic Pathology
Kyoto University Hospital
54 Shogoin Kawaracho, Sakyo
Kyoto 606-8507, Japan
Email: yyamada@kuhp.kyot-u.ac.jp
Fax: +81-75-751-3499
Tel: +81-75-751-4946

**Abbreviations:** None declared

**ABSTRACT (150 words)**

Even though it is a rare subtype, identifying the genetic features of thymic adenocarcinoma is valuable for a multifaceted understanding of thymic epithelial tumors. We experienced a female patient with thymic adenocarcinoma associated with thymic cysts. The tumor consisted of a solid whitish lesion (lesion-1) and a large cystic lesion with small papillary nodules (lesion-2). Microscopically, lesion-1 exhibited poorly differentiated adenocarcinoma accompanying numerous inflammatory cell infiltrates, and lesion-2 (the nodules within the cystic lesion) exhibited enteric-type adenocarcinoma. Consistent with the histological difference, whole-exome sequencing revealed that these two components exhibited distinct genetic features, except for only a few shared mutations, including *CDKN2A* truncation. Lesion-1 exhibited microsatellite instability-high signature with high mutation burden, for which immune checkpoint inhibitors might apply; and lesion-2 exhibited whole-genome doubling with *KRAS* hotspot mutation. Our case presents novel genetic features of thymic adenocarcinoma and demonstrates that distinct mutational processes can be operative within a single tumor.

**Keywords:**

Thymic adenocarcinoma; thymic cysts; *CDKN2A*; microsatellite instability; whole-genome doubling

45 **MAIN TEXT (1586 words)**

46 **INTRODUCTION**

47 Primary adenocarcinoma rarely occurs in the thymus. Although the molecular features of
48 thymomas and thymic squamous cell carcinoma (the most common subtype of thymic
49 carcinoma) are becoming clearer (1-3), those of thymic adenocarcinoma remain poorly
50 understood, and this has hindered the establishment of personalized treatment for these
51 patients. Here, we report a unique case of primary thymic adenocarcinoma exhibiting
52 markedly bidirectional progression based on distinct genetic-phenotypic abnormalities.

53

54 **CLINICAL SUMMARY**

55 A 39-year-old female patient without pertinent previous and family history consulted a
56 physician for her clubbed finger and bilateral hand edema. Because no clinical findings
57 suggesting collagen diseases were recognized, the symptoms were suspected to be due to
58 respiratory diseases. She underwent chest X-ray and computed tomography (CT), which
59 revealed a mediastinal tumor. She was hospitalized in our institution for further investigation.
60 Magnetic resonance imaging (MRI) exhibited a 19 cm mass consisting of 12 cm cystic and 7
61 cm solid components in her anterior mediastinum, adjacent to the left side of her heart
62 (Figure S1a). 18F-fluorodeoxyglucose-positron emission tomography (FDG-PET)/CT
63 revealed strongly elevated FDG uptake in the solid component (Figure S1b). Clinical

differential diagnoses included mature teratoma, cystic thymoma, lymphoma, and solitary fibrous tumor. No clinical findings suggesting a metastatic tumor were detected. The tumor was surgically resected with partial resection of the upper lobe of her left lung. She received postoperative radiotherapy (50 Gy/25 fr) and has remained disease-free for approximately two years.

## PATHOLOGICAL FINDINGS

The macroscopic finding of the resected tumor was almost consistent with the radiographic findings. The tumor consisted of a whitish solid mass measuring 7.5 cm, with expansile invasion to the adjacent lung, and a unilocular cyst measuring 14 cm, filled with brownish mucous material. The inner wall of the cyst was not totally smooth, but contained two small papillary nodules, measuring 1.7 cm and 1.0 cm (Figure S1c-e).

Microscopically, the solid mass consisted of poorly differentiated adenocarcinoma with geographic necrosis (Figure 1a) (henceforth lesion-1). The tumor cells had sizeable nuclei with distinct nucleoli and abundant eosinophilic cytoplasm. They proliferated, showing mainly solid but sometimes tubular or (micro)papillary patterns (Figure 1b-c). Many mature lymphocytes and plasma cells were present in the tumor (Figure 1d). No cystic wall surrounding the solid component was evident.

The papillary nodules within the cyst exhibited well- to moderately differentiated

adenocarcinoma (Figure 2a) (henceforth lesion-2). The tumor cells had a clearer cytoplasm (Figure 2b), and some contained intracellular mucin (Figure 2c). The other parts of the cyst were lined with mucinous epithelium with variable cytological atypia (Figure 2d). Immunohistochemically, the tumor cells in lesion-1 were positive for pan-cytokeratin (CK) and CD5 and negative for CD117, CDX2, p40, SATB2, and TTF1 (Figure 3a-d). The carcinoma cells in lesion-2 were also CK (+)/CD5 (+)/CD117 (-)/TTF1 (-), but partly positive for CDX2 and SATB2, consistent with morphological enteric differentiation (Figure 4a-c). CD30, CK20, MUC2, and SALL4 were negative in both tumor components (not shown).

Around the macroscopic cyst, several small cysts lined with mucinous epithelium without significant atypia in addition to an atrophic non-neoplastic thymus were observed (Figure S2a-c). Considering all findings, we diagnosed the case as enteric-type adenocarcinoma of the thymus (4) with a poorly differentiated component, associated with thymic cysts.

Although both lesions (i.e., poorly differentiated adenocarcinoma in the solid lesion [lesion-1] and well-differentiated adenocarcinoma in the cystic lesion [lesion-2]) were not directly connected microscopically, we hypothesized that the poorly differentiated component (lesion-1) had developed from the well-differentiated component (lesion-2) through tumor progression (Figure 5a). We then performed WES for lesion-1 and lesion-2 independently, expecting to find genetic features related to the initiation and progression of thymic

adenocarcinoma. We used an R package, deconstructSigs (v. 1.9.0), to decompose the mutational signatures. COSMIC Mutational Signatures Version 3.0 was used.

Our hypothesis was “partially” correct. WES revealed that both lesions shared nine mutations, including a *CDKN2A* truncating mutation. Copy number analysis identified shared features including 6q loss, 9 loss (resulting in loss of heterozygosity [LOH] in *CDKN2A*), and 18q loss, further supporting that they were derived from a common ancestor (Figure 5b). Consistent with the genetic findings, both lesions were completely negative for p16 protein in immunohistochemistry (IHC) (Figure 3e and 4d).

Two lesions exhibited distinct genetic features, albeit derived from a common ancestor; the solid lesion (lesion-1) harbored 203 indels and 912 single nucleotide variations (SNVs), including *TSC1*, *ARID1B*, and *ARID1A*. Lesion-1 showed a high indel/SNV ratio, and the signature analysis suggested evidence of COSMIC signature 15 (attributed to microsatellite instability) as well as signature 1 (attributed to aging) (Figure 5b and S3). These results suggested lesion-1 was a microsatellite instability-high (MSI-H) carcinoma; indeed, the tumor cells showed loss of MLH1 protein expression in IHC (Figure 3f). In contrast, the carcinoma within the cyst (lesion-2) carried far fewer mutations (3 indels / 34 SNVs) as compared to the solid part (lesion-1) and carried a likely driver mutation, *KRAS G12D* (Figure 5b). Further, copy number analysis suggested whole-genome doubling, resulting in tetraploidy (Figure 5c). These results indicate that both the poorly differentiated

(lesion-1) and well-differentiated (lesion-2) lesions developed from a common ancestor with *CDKN2A* inactivation, but followed distinct evolutionary trajectories that resulted in different phenotypes.

## DISCUSSION

Recent studies, including one conducted as a part of the Cancer Genome Atlas (TCGA) project, have advanced our understanding of the genetic features of thymic epithelial tumors (TETs). Chromosomal loss of 6q25.2-q25.3 can occur in TETs across histotypes. *GTF2I L242H* mutation is the most frequent in type A/AB thymomas. In thymic squamous cell carcinoma, loss of 16q is a common event, and several oncogenic mutations, such as those of *CYLD*, *TP53*, or *KIT,* may be observed, although no recurrent mutations are known (1-4).

To date, however, only a few English-language reports have described the genetic abnormalities of thymic adenocarcinoma (5-7). As such, our case exhibited several novel genetic features, namely, *CDKN2A* mutations/deletions, an MSI-H phenotype, and whole-genome doubling.

*CDKN2A* is one of the commonly affected tumor suppressor genes across cancer types (8, 9) and can involve tumor predisposition, initiation, and progression (10). Accordingly, it is reasonable to think that this is one of the earliest events for (both components of) the tumor in our case and possibly occurred in the epithelium of the thymic

cysts. It was technically challenging to determine the mutation status of *CDKN2A* of the benign-looking epithelium of the cysts surrounding the two cancerous lesions. Considering that the epithelium was positive for p16, albeit very focally (Figure S2c-d), these thin cysts may harbor wild-type *CDKN2A*, and the common ancestor of the two cancers may have become effaced through the tumor progression. The TCGA 'Thymoma' dataset (that also comprised thymic carcinomas, however, no adenocarcinomas) detected the homozygous deletion of *CDKN2A* in approximately 4% of thymic epithelial tumors across histotypes (2, 8, 9), suggesting this abnormality may be a common finding in thymic epithelial tumors.

The second novel genetic feature is the MSI-H phenotype, which the poorly differentiated adenocarcinoma of the solid lesion exhibited. Because no apparent mutations of DNA mismatch repair genes, including *MLH1*, were detected in either lesion, we think that the loss of MLH1 protein expression in lesion 1 was caused by epigenetic changes, such as *MLH1* promoter methylation. MSI-H is a common cancer phenotype observed in many cancers (11). MSI-H cancers are well-known to exhibit a better response to immune checkpoint inhibitors, especially when the tumor mutation burden is high, as in our case (12). In the TCGA dataset, one among nine thymic carcinomas exhibited the MSI-H phenotype (the diagnosis was undifferentiated carcinoma) (2), and, to the best of our knowledge, our case is the second reported case of MSI-H thymic carcinoma. Considering that a previous comprehensive study (2) and our signature analysis did not reveal any predisposing factors

(e.g., smoking and ultraviolet) for thymic epithelial tumors, the MSI-H phenotype might be a more prevalent feature of thymic carcinoma than expected.

The third novel genetic feature is whole genome doubling (WGD), which was detected in the intracystic adenocarcinoma (lesion-2). WGD is a common event in many cancers, and has both prognostic and therapeutic relevance, because a recent study reported that WGD (+) cells exhibited a unique dependence on particular signaling pathways (e.g., those related to the spindle-assembly checkpoint) and vulnerability for loss of KIF18A (13). Lopez et al. reported that WGD is enriched in tumor types with extensive LOH and suggested that it occurs to mitigate the accumulation of deleterious somatic alterations (14). We wonder if the simple columnar epithelium surrounding the enteric-type adenocarcinoma (lesion 2) might show the genetic state before WGD. This hypothesis could not be addressed by WES of the columnar epithelial cells due to their insufficient number.

Altogether, our case suggests that thymic adenocarcinoma can develop through relatively common genetic abnormalities rather than unique mutations, such as the mostly type A/AB thymoma-specific *GTF2I L424H* mutation (1). Therefore, targeted therapies that apply to cancers in other organs might be feasible. Also, our case likely expands the concept of the branched evolution model of cancer (15); the two components of the tumor followed distinct trajectories with different therapeutic implications.

Recently, gene panel testing is becoming routine for unresectable tumors. Our case

178 underscores the importance of cautious histological evaluation for heterogeneous tumors in
179 that morphologically different components can exhibit more distinct, potentially druggable,
180 genetic abnormalities than expected. If a test is performed with only one histological
181 component or with a bulk sample, precise genetic information may not be obtained and may
182 lead to suboptimal treatments.

183 Our case presents novel genetic features of thymic adenocarcinoma, which illustrates
184 a unique process of tumor evolution, and suggests caution in tissue-based genetic testing.

185

186

## FIGURE LEGENDS

**Figure 1. Histological findings of the solid lesion of the thymic adenocarcinoma (lesion-1).**

The tumor exhibits geographic necrosis (panel a). The tumor cells have sizeable nuclei with distinct nucleoli and a wide eosinophilic cytoplasm; they exhibit mainly solid (panel b) but sometimes tubular or (micro)papillary patterns (panel c). Many mature lymphocytes and plasma cells are present in the tumor (panel d) (hematoxylin and eosin section).

**Figure 2. Histological findings of the cystic lesion of the thymic adenocarcinoma (lesion-2).**

The papillary nodules within the cyst exhibit well-differentiated adenocarcinoma (panel a). The tumor cells have a clearer cytoplasm (panel b), and some contain intracellular mucin (panel c). The other parts of the cyst are lined with mucinous epithelium with variable cytological atypia (panel d) (hematoxylin and eosin section).

**Figure 3. Immunohistochemical findings of the solid lesion of the thymic adenocarcinoma (lesion-1).**

The tumor cells are positive for CD5 (panel a) and negative for CDX2 (panel b), SATB2 (panel c), p40 (panel d), p16 (panel e), and MLH1 (panel f) (immunohistochemistry).

**Figure 4. Immunohistochemical findings of the cystic lesion of the thymic adenocarcinoma (lesion-2).**

The tumor cells are positive for CD5 (panel a), CDX2 (panel b), SATB2 (panel c), and negative for p16 (panel d) (immunohistochemistry).

**Figure 5. Whole-genome sequencing of the thymic adenocarcinoma**

The scheme of the tumor (panel a). Mutations detected in the solid (lesion-1) and cystic (lesion-2) components (panel b). Few mutations, including *CDKN2A*, are shared between the two lesions. Lesion-1 harbors numerous mutations (>900/exome), including *TSC1*, *ARID1B*, and *ARID1A*. Lesion-2 harbors relatively fewer mutations but has *KRAS G12D*. Copy number analysis for both lesions (panel c). Lesion-2 mostly exhibits the tetraploid karyotype, suggesting whole-genome doubling.

## SUPPLEMENTAL INFORMATION

**Figure S1. Radiologic and macroscopic findings of the thymic adenocarcinoma.**

T2-weighted magnetic resonance imaging (MRI) exhibited a large cystic lesion and a smaller solid lesion on the left side of the anterior mediastinum (panel a). 18F-fluorodeoxyglucose-positron emission tomography (FDG-PET)/CT revealed strongly elevated FDG uptake in the solid component (panel b). Macroscopic findings of the tumor (panel b-d). A solid whitish lesion pushing the adjacent lung is observed (panels c and d). The cystic lesion is filled with brownish mucous material but contains small papillary nodules (panel e).

**Figure S2. Microscopic findings of the thymic adenocarcinoma.**

Microscopic findings around the macroscopic cystic tumor (T) (panels a and b). Small cysts lined with mucinous epithelium without significant atypia (C) (panel a) and non-neoplastic atrophic thymus (Thy) (panel b) and are observed. The epithelium of the benign-looking cysts (C) was very focally positive for p16 (panel c and d) (a-c: hematoxylin and eosin section, d: immunohistochemistry).

**Figure S3. Whole-genome sequencing of the thymic adenocarcinoma.**

The solid lesion (lesion-1) harbors numerous mutations (> 900/exome) with a high indel/SNV

240 ratio, and the signature analysis reveals a strong influence of Signature 15 (Microsatellite
241 instability) and Signature 1 (Aging).
242

## DECLARATIONS

**Conflicts of interest**: None declared

**Authors' contributions:**

Drafting the manuscript and figures: AI, YI, and YY. Acquisition and analysis of genetic data: YI. Acquisition and analysis of clinical data: DN and HD. Correction and approval of the manuscript: all authors.

**Ethics approval:**

The project was approved by an institutional ethics committee.

## REFERENCES

1. Petrini I, Meltzer PS, Kim IK, et al. A specific missense mutation in GTF2I occurs at high frequency in thymic epithelial tumors. Nat Genet. 2014;**46**:844-9.
2. Radovich M, Pickering CR, Felau I, et al. The Integrated Genomic Landscape of Thymic Epithelial Tumors. Cancer Cell. 2018;**33**:244-58.e10.
3. Yamada Y, Simon-Keller K, Belharazem-Vitacolonnna D, et al. A tuft cell-like signature is highly prevalent in thymic squamous cell carcinoma and delineates new molecular subsets among the major lung cancer histotypes. J Thorac Oncol. 2021;**16**:1003-1016
4. WHO Classification of Tumours Editorial Board. Thoracic tumours. Lyon (France): International Agency for Research on Cancer; 2021.
5. Lee Y, Park S, Lee SH, Lee H. Characterization of genetic aberrations in a single case of metastatic thymic adenocarcinoma. BMC Cancer. 2017;**17**:330.
6. Maghbool M, Ramzi M, Nagel I, et al. Primary adenocarcinoma of the thymus: an immunohistochemical and molecular study with review of the literature. BMC Clin Pathol. 2013;**13**:17.
7. Sakanoue I, Hamakawa H, Fujimoto D, et al. KRAS mutation-positive mucinous adenocarcinoma originating in the thymus. J Thorac Dis. 2017;**9**:E694-E7.
8. Cerami E, Gao J, Dogrusoz U, et al. The cBio cancer genomics portal: an open platform for exploring multidimensional cancer genomics data. Cancer Discov. 2012;**2**:401-4.
9. Gao J, Aksoy BA, Dogrusoz U, et al. Integrative analysis of complex cancer genomics and clinical profiles using the cBioPortal. Sci Signal. 2013;**6**:pl1.
10. Kakiuchi N, Ogawa S. Clonal expansion in non-cancer tissues. Nat Rev Cancer. 2021;**21**:239-56.
11. Cancer Genome Atlas Newwork. Comprehensive molecular characterization of human colon and rectal cancer. Nature. 2012;**487**:330-7.
12. Schrock AB, Ouyang C, Sandhu J, et al. Tumor mutational burden is predictive of response to immune checkpoint inhibitors in MSI-high metastatic colorectal cancer. Ann Oncol. 2019;**30**:1096-103.
13. Quinton RJ, DiDomizio A, Vittoria MA, et al. Whole-genome doubling confers unique genetic vulnerabilities on tumour cells. Nature. 2021;**590**:492-7.
14. López S, Lim EL, Horswell S, et al. Interplay between whole-genome doubling and the accumulation of deleterious alterations in cancer evolution. Nat Genet. 2020;**52**:283-93.
15. Gerlinger M, Rowan AJ, Horswell S, et al. Intratumor heterogeneity and branched evolution revealed by multiregion sequencing. N Engl J Med. 2012;**366**:883-92.

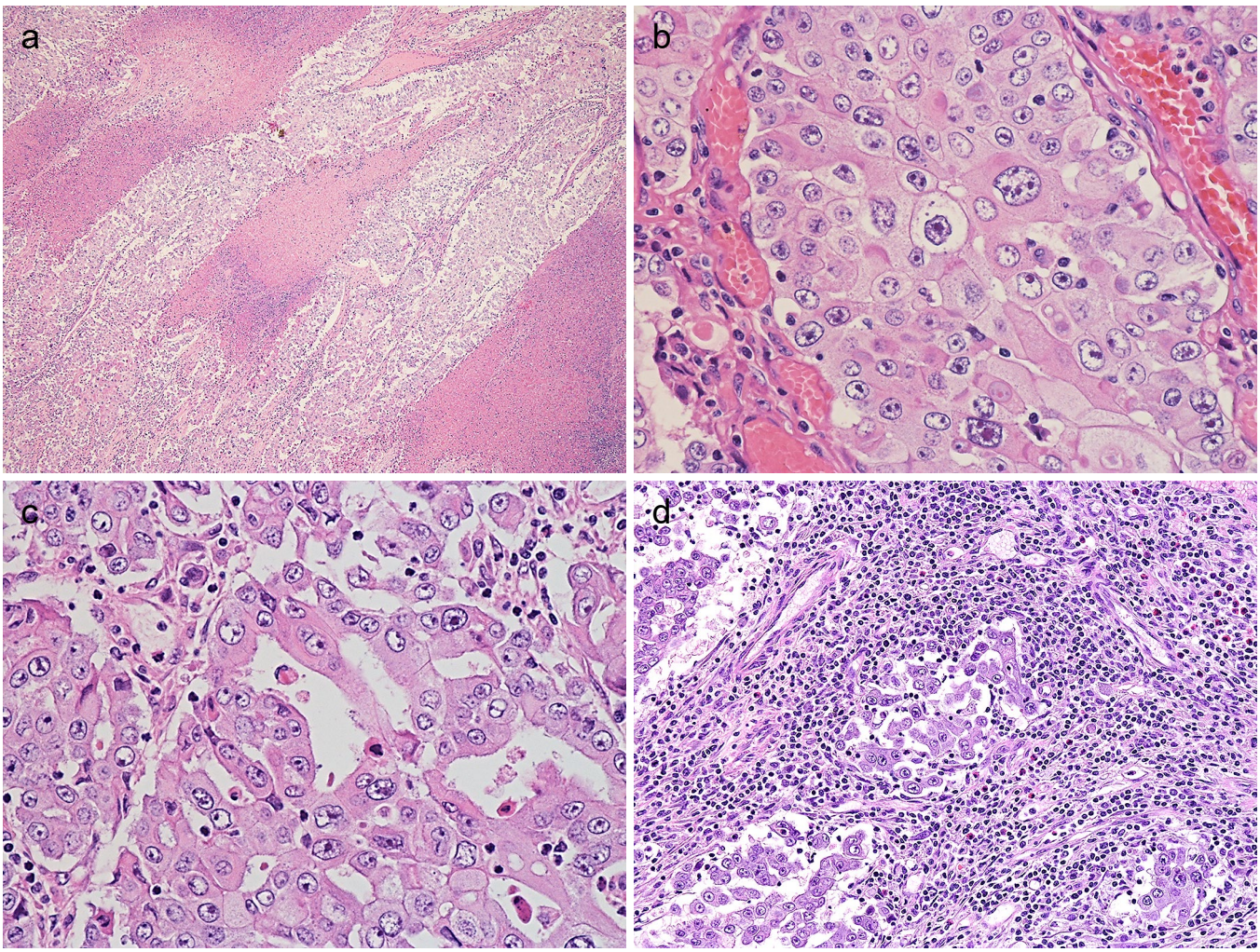

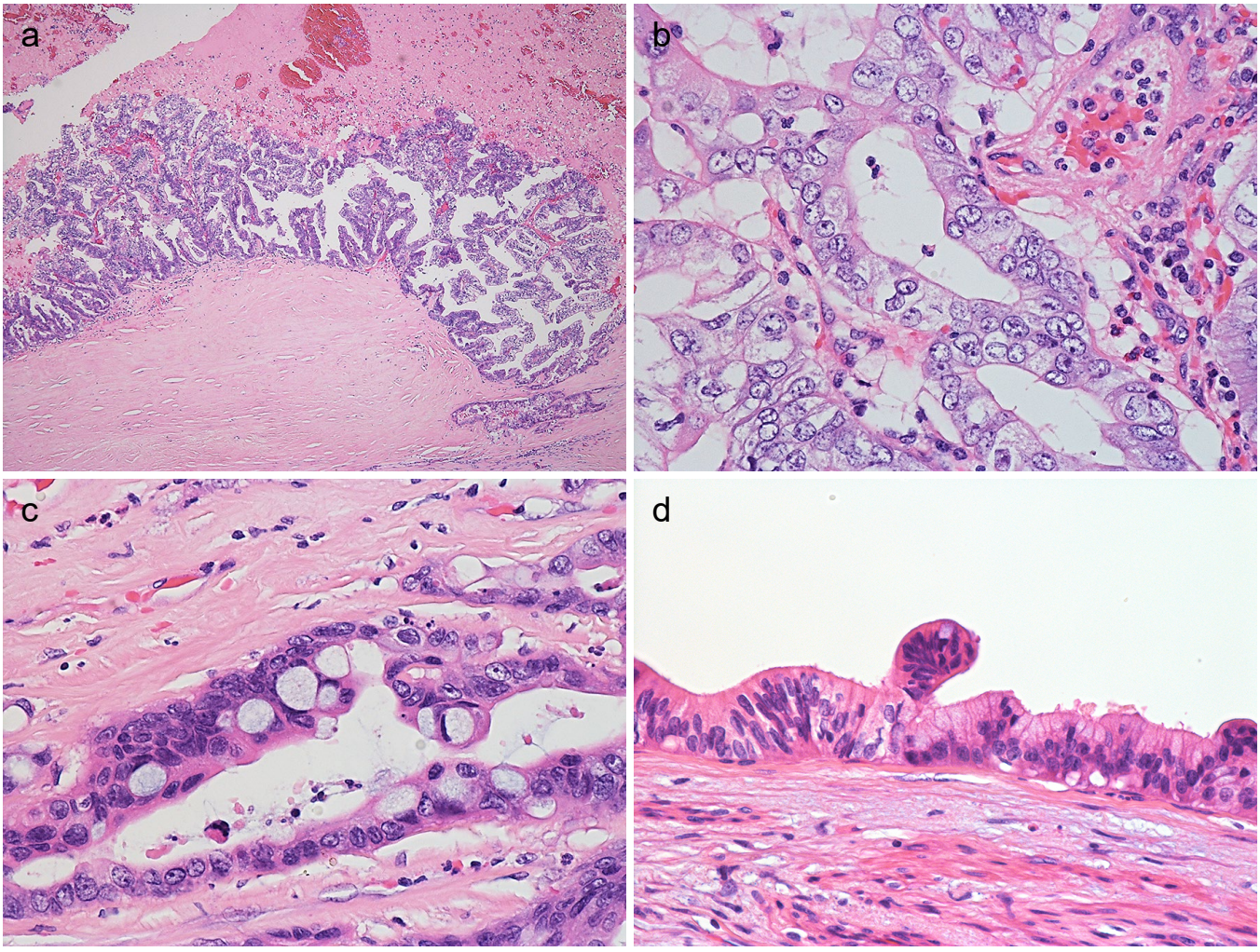

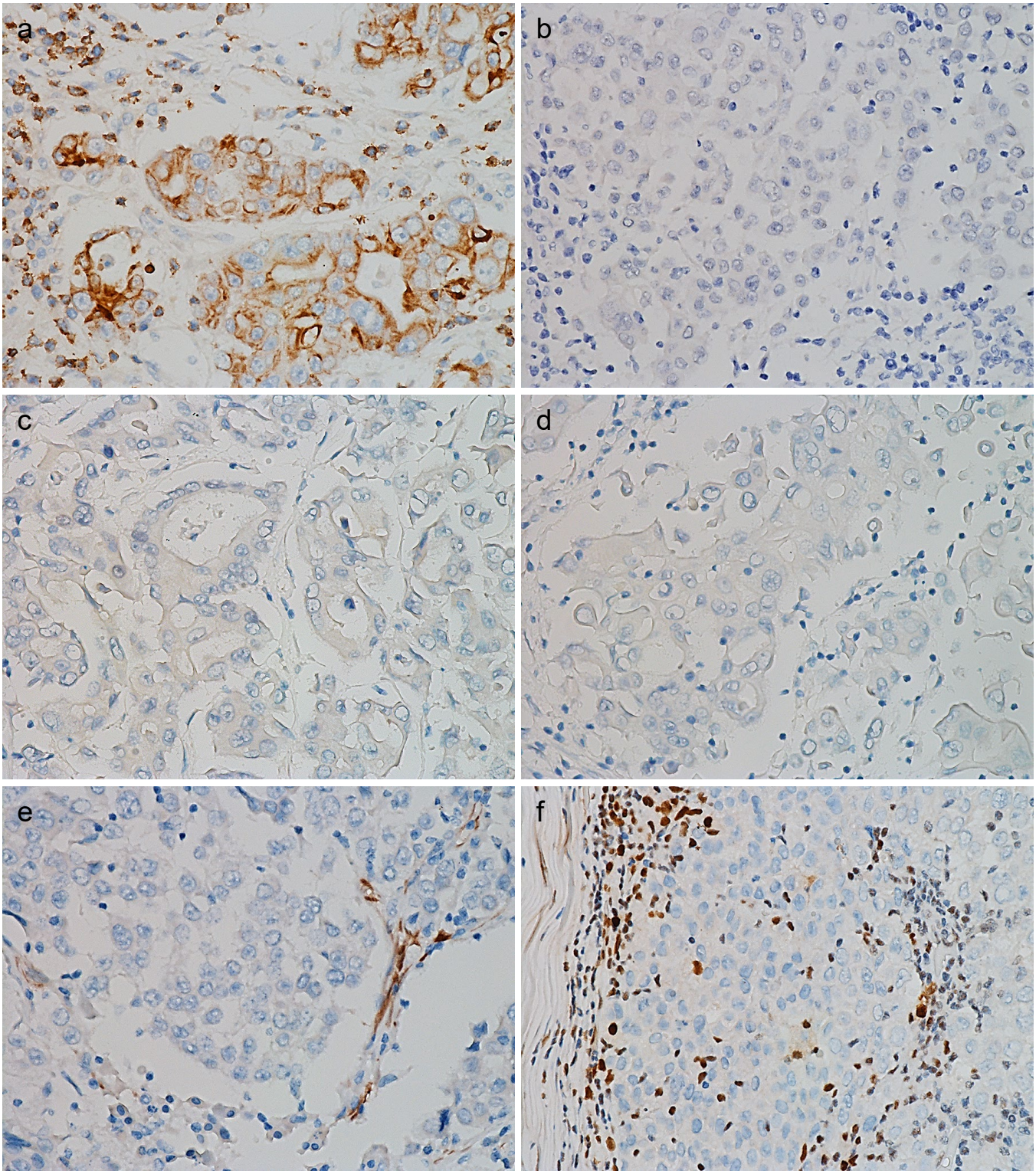

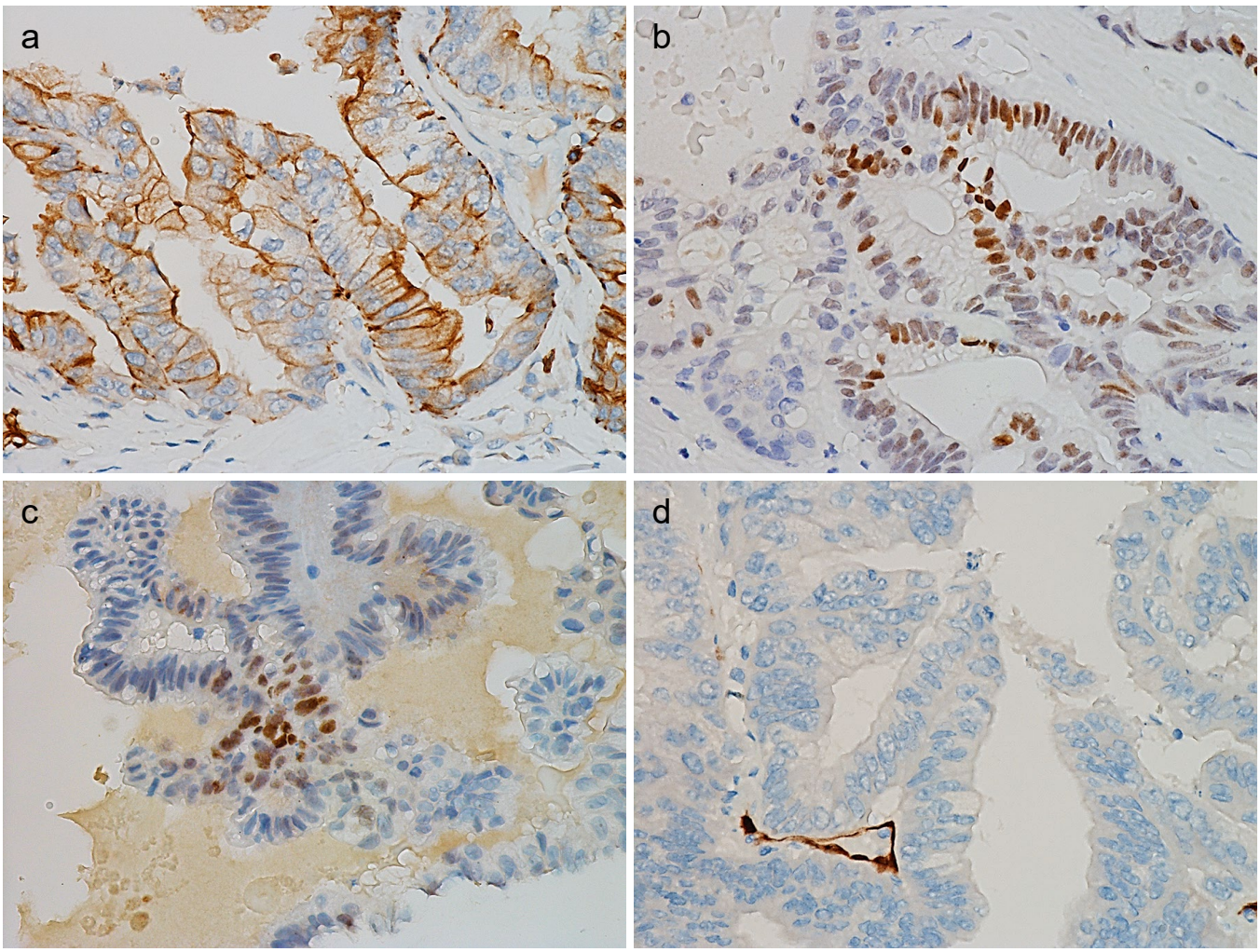

a. The scheme of the tumor

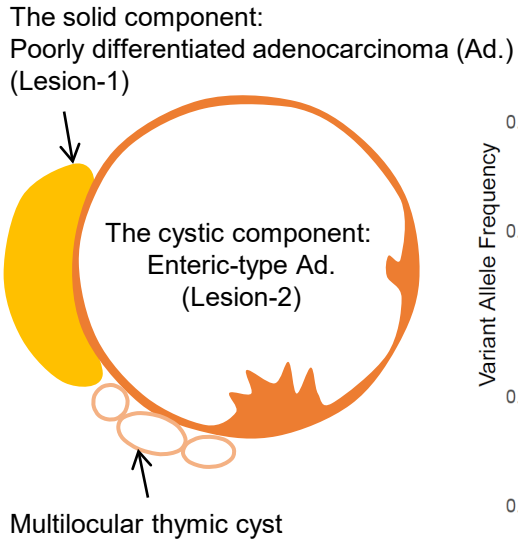


b. Observed genetic mutations

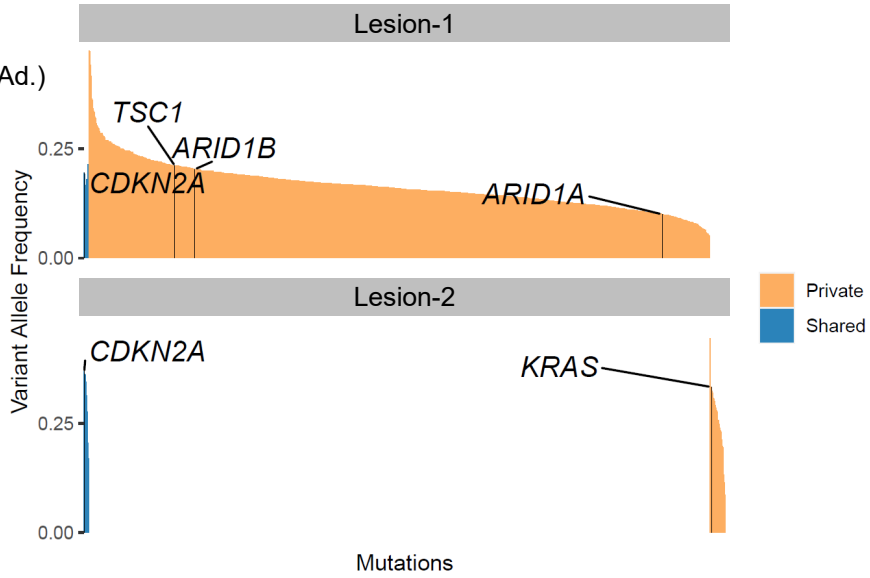


c. Copy number analysis

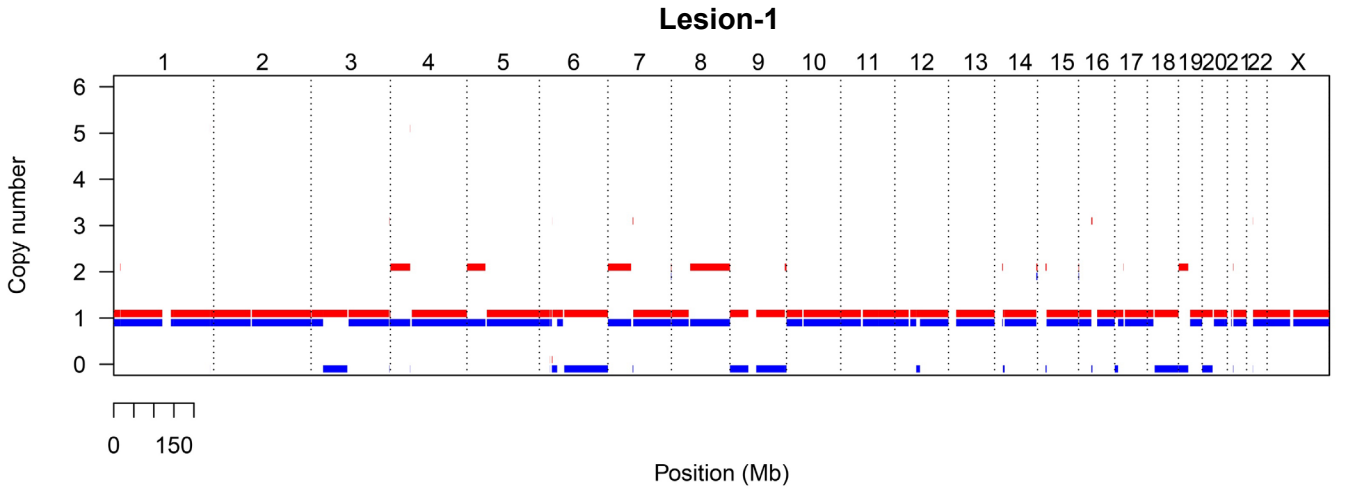


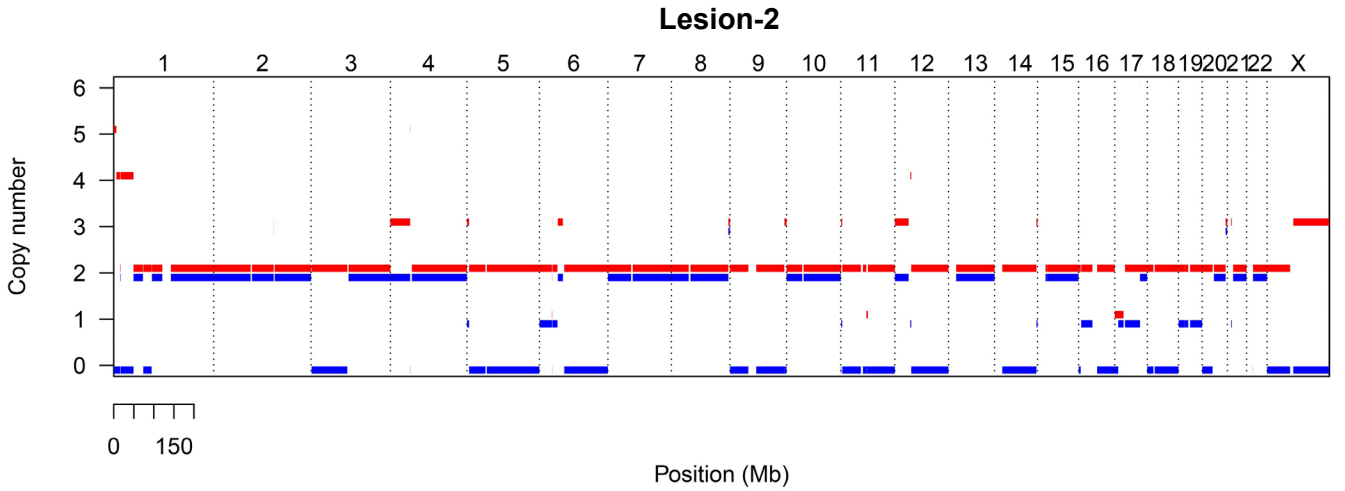

# Figure S1

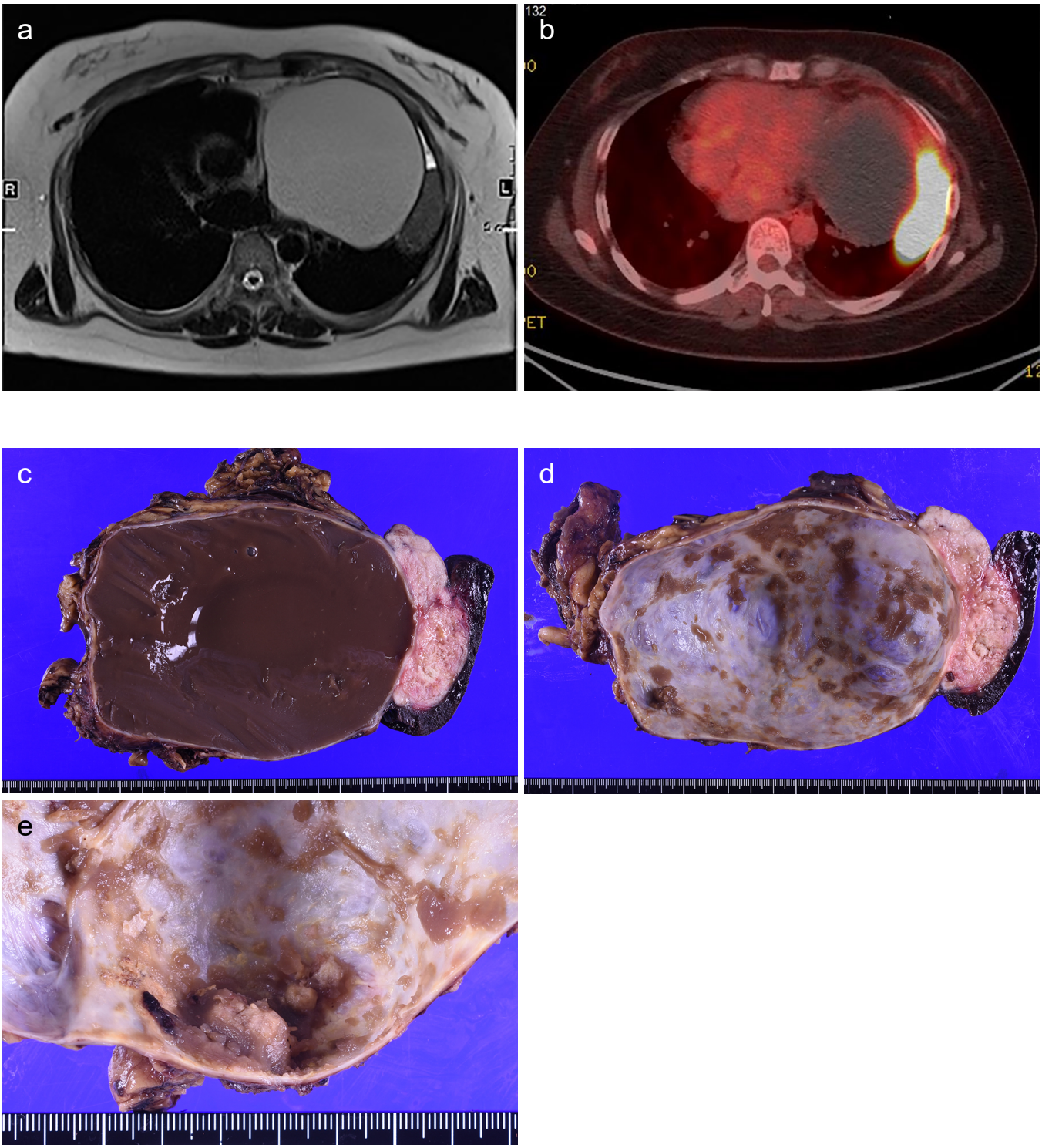


c



d



e

Figure S2

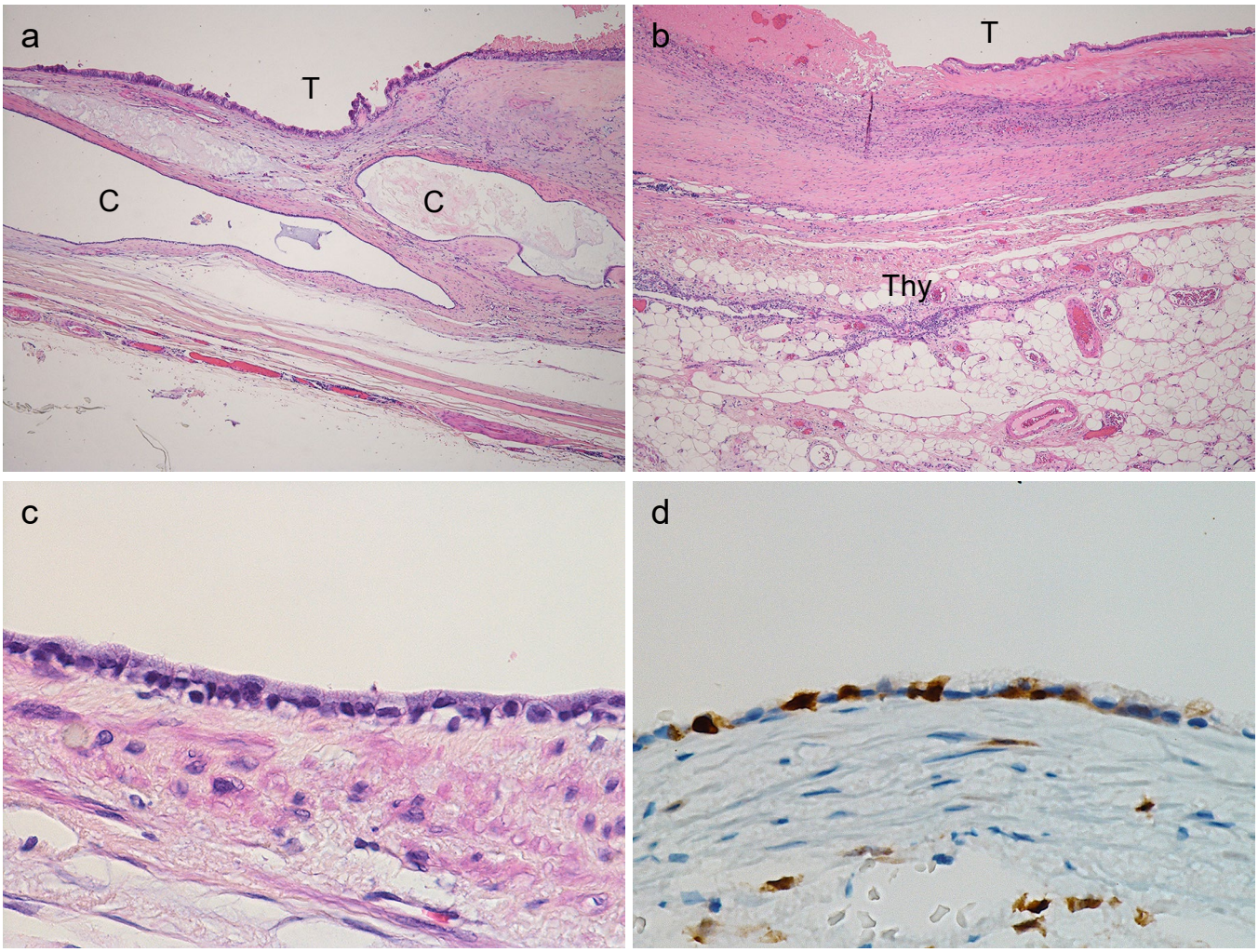

Figure S3